Published in final edited form as:
Immunity. 2007 August ; 27(2): 253–267.

TRAF3 is a critical regulator of B cell homeostasis in secondary lymphoid organs

Ping Xie[1], **Laura L. Stunz**[1], **Karen D. Larison**[1], **Baoli Yang**[3], and **Gail A. Bishop**[1,2,4]

1*Departments of Microbiology, The University of Iowa, Iowa City, IA 52242.*

2*Internal Medicine, The University of Iowa, Iowa City, IA 52242.*

3*Obstetrics and Gynecology, The University of Iowa, Iowa City, IA 52242.*

4*Veterans Affairs Medical Center, Iowa City, IA 52242.*

Summary

TRAF3 is an adaptor protein that directly binds to a number of receptors of the tumor necrosis factor receptor (TNF-R) superfamily. Despite *in vitro* evidence that TRAF3 plays diverse roles in different cell types, little is known about the *in vivo* functions of TRAF3. To address this gap in knowledge and to circumvent the early lethal effect of TRAF3 null mutations, we generated conditional TRAF3-deficient mice. B cell-specific TRAF3$^{-/-}$ mice displayed severe peripheral B cell hyperplasia, which culminated in hyperimmunoglobulinemia, increased T-independent antibody responses, splenomegaly and lymphadenopathy. Resting splenic B cells from these mice exhibited remarkably prolonged survival *ex vivo* independent of BAFF, and showed increased levels of nuclear NF-κB2 but decreased levels of nuclear PKCδ. Furthermore, these mice developed autoimmune manifestations as they aged. These findings indicate that TRAF3 is a critical regulator of peripheral B cell homeostasis and may be implicated in the regulation of peripheral self-tolerance induction.

Introduction

TNF-R-associated factor 3 (TRAF3), a member of the TRAF family of cytoplasmic adaptor proteins, is exploited for signaling by a number of receptors of the TNF-R superfamily as well as the Epstein-Barr virus (EBV)-encoded oncoprotein latent membrane protein 1 (LMP1) (Bishop, 2004; Miller et al., 2006; Wajant et al., 2001). TRAF3 directly binds to almost all TNF-R superfamily receptors that do not contain death domains, including CD40, receptors for BAFF and APRIL, LTβR, CD27, CD30, RANK, HVEM, EDAR, XEDAR, 4-1BB, OX-40, and GITR. Among these, BAFF receptors and CD40 are pivotal in the physiology of B lymphocytes, the only mammalian cell type that can produce antibodies.

BAFF is a crucial B cell survival factor, binding to three receptors of the TNF-R superfamily: BCMA, TACI, and BAFF-R (Mackay et al., 2003; Miller et al., 2006). TACI and BCMA are also bound by APRIL, a TNF family member closely related to BAFF. Interestingly, BAFF-R appears to be the sole mediator of BAFF-mediated B cell survival signals. Only BAFF-R$^{-/-}$ mice recapitulate the phenotype of BAFF$^{-/-}$ mice, which display almost complete loss of

Address correspondence to: Gail A. Bishop, 2193B MERF, Dept. of Microbiology, University of Iowa, Iowa City, IA 52242, Phone: (319) 335-7945, Fax: (319) 335-9006, E-mail: gail-bishop@uiowa.edu.

Competing interests statement
The authors declare that they have no competing financial interests.

mature B lymphocytes and marginal zone B cells, and deficiency in mounting T-dependent humoral responses (Schiemann et al., 2001; Shulga-Morskaya et al., 2004). In contrast, B cell maturation in BCMA$^{-/-}$, TACI$^{-/-}$, and BCMA$^{-/-}$ TACI$^{-/-}$ mice is normal or enhanced (Mackay et al., 2003; Shulga-Morskaya et al., 2004). The two predominant signaling pathways initiated by BAFF/BAFF-R interactions shown to promote B cell survival are the alternative NF-κB (NF-κB2) pathway and inhibition of PKCδ nuclear translocation (Claudio et al., 2002; Mecklenbrauker et al., 2004). To date, the only TRAF protein shown to directly interact with BAFF-R is TRAF3 (Miller et al., 2006). A recent study reported that mutation of the putative TRAF-binding motif of BAFF-R abolishes its interaction with TRAF3 and its ability to induce NF-κB2 activation in the mouse B cell line M12, suggesting that TRAF3 is critical for BAFF-R-mediated NF-κB2 activation in B cells (Morrison et al., 2005).

CD40 and its ligand CD154 are obligatory for T cell-dependent B cell activation, regulating formation of germinal centers, immunoglobulin (Ig) isotype switching, and development of memory B cells (Bishop, 2004; Quezada et al., 2004). All these processes are severely impaired in CD40$^{-/-}$ or CD154$^{-/-}$ mice, or in human patients carrying CD154 mutations (Grammer and Lipsky, 2000). Upon ligand binding, CD40 recruits TRAF1, 2, 3, 5 and 6, directly or indirectly to its signaling complex (Bishop, 2004; Grammer and Lipsky, 2000; Xie et al., 2006). TRAF recruitment in turn triggers multiple signaling cascades, including activation of kinases (such as p38, JNK, ERK, and Akt) and transcription factors (such as NF-κB and AP-1). This ultimately leads to proliferation, upregulation of adhesion and co-stimulatory molecules, and secretion of antibodies and cytokines (Bishop, 2004; Grammer and Lipsky, 2000). Using TRAF3$^{-/-}$ B cell lines, we previously showed that CD40-induced JNK activation and antibody secretion are enhanced in the absence of TRAF3 (Xie et al., 2004). Conversely, signaling by the viral oncogenic mimic of CD40, LMP1, is defective in TRAF3$^{-/-}$ B cells (Xie and Bishop, 2004; Xie et al., 2004). LMP1-induced activation of JNK, p38 and NF-κB, upregulation of CD23 and CD80, as well as antibody secretion are profoundly impaired by TRAF3 deficiency (Xie and Bishop, 2004; Xie et al., 2004). Thus, CD40 and LMP1 use TRAF3 in sharply different ways in B cells.

In addition to directly interacting with the TNF-R superfamily receptors, TRAF3 has recently been found to be involved in production of type I interferon and IL-10 induced by Toll-like receptors (TLRs) in macrophages and dendritic cells through association with TRIF, an adaptor protein for TLRs (Hacker et al., 2006; Oganesyan et al., 2006). Taken together, these *in vitro* observations indicate that TRAF3 can play important and diverse roles depending on the specific interacting receptor and cellular context. This warrants further *in vivo* investigation to understand the physiological functions of TRAF3 in the intact animal.

Mice genetically deficient in TRAF3 die within 10 days after birth, demonstrating the ubiquitous and critical developmental functions of TRAF3 (Xu et al., 1996). However, assessment of specific functions of TRAF3 in the immune system and in signaling by the TNF-R superfamily/TLRs in tissues of adult mice is compromised by the early lethality of TRAF3$^{-/-}$ mice. To circumvent this problem, we employed a conditional gene targeting strategy through Cre-loxP-mediated recombination and generated conditional TRAF3-deficient mice, which allow the deletion of the TRAF3 gene in specific cell types or tissues. We found that specific ablation of TRAF3 in the B cell lineage led to remarkably prolonged B cell survival and greatly expanded B cell compartments in secondary lymphoid organs with markedly increased numbers of T2 transitional, marginal zone and follicular B cells. This culminated in splenomegaly and lymphadenopathy, hyperimmunoglobulinemia, and autoimmune reactivity. Our findings reveal a novel role for TRAF3 in regulating peripheral B cell homeostasis, and implicate TRAF3 as playing an important role in peripheral self-tolerance induction.

Results

Conditional deletion of the TRAF3 gene

Using a conditional gene targeting approach, we generated mouse embryonic stem cells and a new mouse strain in which the TRAF3 gene is modified with insertions of two loxP sequences, recognition sites of the DNA recombinase Cre, into the introns flanking the first two coding exons of TRAF3 (Supplementary Fig. 1 and 2). Such "flox" modification of the TRAF3 gene ($TRAF3^{flox}$) does not affect the expression of TRAF3 unless Cre-mediated deletion of the first two coding exons occurs, which leads to a TRAF3 null allele ($TRAF3^{\Delta}$)(Supplementary Fig. 1A). Mice homozygous for the floxed TRAF3 allele ($TRAF3^{flox/flox}$) were fertile and healthy.

To delete the loxP flanked TRAF3 alleles specifically in B lymphocytes, we used a transgenic mouse strain expressing Cre under the control of the endogenous CD19 locus, providing a B cell-specific source of Cre (Rickert et al., 1997). It has been previously shown that $CD19^{Cre}$ mediates deletion of loxP flanked gene segments specifically in the B cell lineage, and that the deletion efficiency is 75-80% in the bone marrow (BM) and >95% in splenic B cells (Pasparakis et al., 2002; Rickert et al., 1997). $TRAF3^{flox/flox}CD19^{+/Cre}$ mice were born at the expected Mendelian frequencies, and survive and breed normally. We verified excision of the first two coding exons of the TRAF3 gene and the elimination of TRAF3 protein expression in splenic B cells of $TRAF3^{flox/flox}CD19^{+/Cre}$ mice (B-$TRAF3^{-/-}$ mice) by genomic PCR and Western blot analysis, respectively (Supplementary Fig. 1C, and Fig. 1A).

Splenomegaly and lymphoadenopathy with expanded B cell compartments in B-$TRAF3^{-/-}$ mice

Adult B-$TRAF3^{-/-}$ mice exhibited greatly enlarged spleens and lymph nodes (LN) compared to those from $TRAF3^{flox/flox}$ littermate control (LMC) mice or wild type mice (Fig. 1B and data not shown). In contrast, the thymus size of B-$TRAF3^{-/-}$ mice was comparable to that of LMC, and spleen size of $TRAF3^{+/flox}CD19^{+/Cre}$ mice was similar to LMC (data not shown). Histochemical staining of LN sections revealed that B-$TRAF3^{-/-}$ mice had increased size and numbers of lymphoid follicles (Supplementary Fig.3A).

To determine which cell types were expanded in the enlarged spleen and LN of B-$TRAF3^{-/-}$ mice, we performed cellularity analysis by immunofluorescence staining and flow cytometry. Proportions and absolute numbers of B cells ($B220^+$ or IgM^+) in both spleen and LN were markedly increased, while the proportion of T cells ($CD3^+$) was reduced in B-$TRAF3^{-/-}$ mice (Fig.1C, Supplementary Table 1). Further detailed analysis of B cell subsets revealed that the numbers of T2 transitional ($B220^+AA4.1^+IgM^+CD23^+$ or $B220^+AA4.1^+IgM^+IgD^+$), follicular ($B220^+IgM^+CD21^{int}CD23^{hi}$) and marginal zone ($B220^+IgM^+CD21^{hi}CD23^{int}$ or $B220^+IgM^+CD1d^+CD9^+$) B cells were vastly increased in the spleen of B-$TRAF3^{-/-}$ mice (Fig. 1D and 1E, Supplementary Fig. 3B and Table 1). Particularly, both the percentage and number of marginal zone B cells were increased in B-$TRAF3^{-/-}$ mice, and such an expansion of marginal zone B cells was also verified by immunofluorescence staining of spleen cryosections (Supplementary Fig. 6). Interestingly, the expression levels of CD21 and CD23, two markers for peripheral B cell maturation, were increased in both splenic and LN B cells of B-$TRAF3^{-/-}$ mice (Supplementary Fig. 4). However, proportions of B-1a ($B220^+CD11b^+CD5^+$), B-1b ($B220^+CD11b^+CD5^-$) and B-2 ($B220^+CD11b^-CD23^+$) subsets in peritoneal lavages from B-$TRAF3^{-/-}$ mice were normal compared to LMC (data not shown). In addition, thymic T cell subsets of B-$TRAF3^{-/-}$ mice were unchanged relative to LMC (Supplementary Fig. 5). Thus, the splenomegaly and lymphadenopathy of B-$TRAF3^{-/-}$ mice were due to massive expansion of B cell compartments, and $TRAF3^{-/-}$ B cell expansion was evident from the T2 transitional B cell stage onward. Because TRAF3 ablation specifically

occurred in the B cell lineage but not in non-B cells, we conclude that the B cell hyperplasia observed in B-TRAF3$^{-/-}$ mice is B cell-autonomous.

Spontaneous germinal center (GC) B cells in B-TRAF3$^{-/-}$ mice

We examined splenic microarchitecture of B-TRAF3$^{-/-}$ mice by immunohistochemical staining and microscopy. Consistent with flow cytometric data, B-TRAF3$^{-/-}$ mice had enlarged white pulp with expanded B cell follicles compared to LMC mice (Fig. 2A). However, the overall organization of B cell follicles (IgM^{+}, blue), T cell zones (CD3^{+}, red) and GC (PNA^{+}, green) were otherwise normal in B-TRAF3$^{-/-}$ mice immunized with sheep red blood cells (SRBC) (Fig. 2A). Notably, 60% (n=10) of unimmunized B-TRAF3$^{-/-}$ mice manifested numerous spontaneous GCs in the spleen, which were not observed in unimmunized LMC mice (Fig. 2A-2C). Flow cytometric analysis revealed that TRAF3$^{-/-}$ splenic GC B (B220^{+}PNA^{+}) cells expressed higher surface IgM and IgG than LMC B cells (Fig. 2D), and that GC B cells are CD38^{low} and CD95^{high} relative to non-GC B (B220^{+}PNA^{-}) cells in both LMC and B-TRAF3$^{-/-}$ mice (Supplementary Fig. 14).

Hyperimmunoglobulinemia and enhanced T-independent antibody responses in B-TRAF3$^{-/-}$ mice

The primary function of B cells is to produce immunoglobulins. Basal serum Ig isotypes IgM, IgG2a, IgG2b, IgG3 and IgA were elevated 2-5 fold in B-TRAF3$^{-/-}$ mice compared to those observed in LMC as measured by enzyme-linked immunosorbent analysis (ELISA) (Fig. 3A). In contrast, basal serum levels of IgG1 and IgE were unaltered (Fig. 3A). In response to the challenge of a T-independent antigen (T-I Ag), trinitrophenyl (TNP)-Ficoll, B-TRAF3$^{-/-}$ mice developed higher titers of anti-TNP IgM, IgG1, IgG2a, IgG2b and IgG3 antibodies as compared to LMC mice (Fig. 3B). Interestingly, following immunization with a T-dependent (T-D) Ag, TNP-KLH, B-TRAF3$^{-/-}$ mice showed an increased TNP-specific IgM response, but a normal TNP-specific IgG1 response as compared to LMC (Fig. 3C). Thus, T-I antibody responses were increased, but the T-D IgG1 response was unaltered in B-TRAF3$^{-/-}$ mice.

Prolonged survival of TRAF3$^{-/-}$ resting splenic B cells *ex vivo*

Expansion of B cell compartments in secondary lymphoid organs may result from increased output from BM, or enhanced proliferation and/or prolonged lifespan of peripheral B cells. To evaluate which of these contributed to the B cell hyperplasia in B-TRAF3$^{-/-}$ mice, we first analyzed proportions and numbers of B cell precursors in BM. Proportions and numbers of pro-B (B220^{+}IgM^{-}c-Kit^{+}CD25^{-}), pre-B (B220^{+}IgM^{-}c-Kit^{-}CD25^{+}), immature (B220^{+}AA4.1^{+}IgM^{+}IgD^{-}), and recirculating mature (B220^{+}AA4.1^{-}IgM^{+}IgD^{+}) B cells in BM of B-TRAF3$^{-/-}$ mice remained similar to those observed in LMC (Supplementary Fig. 7 and Table 1). These data, together with the evidence that the numbers of T1 transitional B cells were only slightly increased (about 1.4 fold) in B-TRAF3$^{-/-}$ mice (Fig. 1E and Supplementary Table 1), suggest that the increase, if any, in production of immature B cells in the BM of B-TRAF3$^{-/-}$ mice is likely to be quite modest.

We next sought to investigate the survival and proliferation capacity of freshly isolated TRAF3$^{-/-}$ resting splenic B cells *ex vivo*. When cultured *ex vivo* with no treatment, TRAF3$^{-/-}$ resting splenic B cells exhibited greatly expanded survival capacity compared to LMC B cells (Fig. 4A). About 30% of TRAF3$^{-/-}$ B cells remained alive even on day 16 of culture, and BAFF treatment did not further improve their survival (Fig. 4A and data not shown). Analysis of cell cycle distribution by propidium iodide staining and flow cytometry showed that in sharp contrast to LMC B cells, TRAF3$^{-/-}$ B cells did not undergo spontaneous apoptosis *ex vivo* even by day 6 of culture (Fig. 4B). Results from both cell cycle analysis and CFSE-dilution experiments demonstrated an unaltered proliferation response in TRAF3$^{-/-}$ B cells following stimulation with CD40, or CD40 in combination with BCR or IL-4 (Supplementary Fig. 8, and

Fig. 4C). The enhanced CD40-induced proliferation response in TRAF3$^{-/-}$ B cells (Fig. 4A) is likely secondary to their prolonged survival (Fig. 4B). Thus, our data indicate that TRAF3 deficiency does not induce proliferation, but can protect splenic B cells from apoptosis, leading to prolonged survival capacity independent of BAFF.

Lack of involvement of soluble factors in enhanced lifespan of TRAF3$^{-/-}$ B cells

The prolonged survival of TRAF3$^{-/-}$ B cells could not be attributed to higher expression of BAFF receptors or CD40, as expression levels of BAFF-R, TACI, BCMA and CD40 in TRAF3$^{-/-}$ resting splenic B cells, either freshly isolated or after stimulation with BAFF or anti-CD40 Abs, were identical to those detected in LMC B cells (Supplementary Fig. 9 and data not shown). We also evaluated the possibility that death receptor-mediated apoptotic pathways may be generally impaired in the absence of TRAF3. However, Fas-mediated apoptosis in TRAF3$^{-/-}$ B cells was intact, and induction of Fas expression by CD40 stimulation was unaffected by TRAF3 deficiency (Supplementary Fig. 10), indicating that extrinsic apoptotic pathways are not detectably impaired in TRAF3$^{-/-}$ B cells. In addition, results of transwell co-culture experiments showed that co-culture of TRAF3$^{-/-}$ and LMC B cells did not prolong the survival of LMC B cells (Supplementary Fig. 11), and thus exclude the possibility that TRAF3$^{-/-}$ B cells may constitutively produce pro-survival cytokines (such as BAFF or IL-6). Together, these results indicate that prolonged survival of TRAF3$^{-/-}$ B cells is due to changes in intrinsic pathways regulating B cell survival and/or apoptosis.

Increased nuclear NF-κB2 and decreased nuclear PKCδ in TRAF3$^{-/-}$ B cells

Activation of both NF-κB1 and NF-κB2 promotes B cell survival and PKCδ nuclear translocation induces B cell apoptosis (Claudio et al., 2002; Mecklenbrauker et al., 2004; Sasaki et al., 2006). We thus assessed whether TRAF3 deficiency alters these pathways. CD40-induced phosphorylation and degradation of IκBα, the hallmark of NF-κB1 activation, was similar in TRAF3$^{-/-}$ and LMC B cells (Fig. 5A). Similarly, CD40-induced phosphorylation of JNK, p38 and ERK was unaltered in TRAF3$^{-/-}$ B cells (Supplementary Fig. 12). Activation of NF-κB2 requires the processing of the inactive precursor p100 to p52 in the cytosol, which allows the p52/RelB dimer to translocate into the nucleus to activate transcription of target genes. *Ex vivo* culture of purified LMC B cells for 24 hr, equivalent to deprivation of endogenous B cell survival factor(s) such as BAFF (Claudio et al., 2002), resulted in an increase in the cytosolic p100 level and a decrease in nuclear p52 and RelB (Fig. 5B and 5C). In contrast, BAFF stimulation decreased the cytosolic p100, but sharply increased nuclear p52 and RelB in LMC B cells. However, such changes in cytosolic p100 or nuclear p52 and RelB levels induced by deprivation of survival factors or BAFF stimulation were not observed in TRAF3$^{-/-}$ B cells. These cells did remain responsive to CD40 engagement, which further increased nuclear p52 and RelB levels similar to that observed in LMC B cells. Interestingly, TRAF3$^{-/-}$ B cells also displayed lower levels of nuclear PKCδ compared to LMC B cells, although the levels of cytosolic PKCδ were comparable (Fig. 5B and 5C). Thus, TRAF3$^{-/-}$ B cells exhibited markedly increased constitutive activation of NF-κB2 and decreased PKCδ nuclear translocation, which would enhance the survival capacity of these cells.

Independence of TRAF3$^{-/-}$ B cell hyperplasia on BAFF/APRIL signaling

To address whether TRAF3 functions as a downstream negative regulator of BAFF signals to inhibit peripheral B cell survival, we examined the effects of *in vivo* administration of TACI-Ig, a soluble fusion protein that blocks both BAFF and APRIL from binding to their receptors (Gross et al., 2001), in B-TRAF3$^{-/-}$ and LMC mice. Although administration of TACI-Ig effectively reduced the spleen weight and depleted B cells in spleen and LN of LMC mice, it was unable to reduce the spleen weight or B cell numbers in spleen and LN of B-TRAF3$^{-/-}$ mice (Fig. 6). Analysis of B cell subsets indicated that TACI-Ig treatment decreased the

proportions of mature B ($B220^+AA4.1^-$) and especially marginal zone B ($B220^+IgM^+CD21^{hi}CD23^{int}$ or $B220^+IgM^+CD1d^+CD9^+$) cells in LMC, but not in B-TRAF3$^{-/-}$ mice (Fig. 6B). These data indicate that TRAF3$^{-/-}$ B cell hyperplasia does not require BAFF/APRIL binding, suggesting that TRAF3 may constitutively inhibit NF-κB2 activation and promote PKCδ nuclear translocation to induce spontaneous apoptosis in peripheral B cells.

Autoimmune manifestations in B-TRAF3$^{-/-}$ mice

In light of the notion that prolonged survival of B cells may contribute to autoimmune diseases (Gauld et al., 2006; Mackay and Kalled, 2002), the spontaneous GC formation in B-TRAF3$^{-/-}$ mice (Fig. 2) prompted us to evaluate whether these mice develop autoimmune diseases. Interestingly, 80% (n=10) of B-TRAF3$^{-/-}$ mice already displayed anti-dsDNA autoantibodies in sera at an early age (10-12 weeks), which were not detected in any LMC mice (n=10) (Fig. 7A and Supplementary Fig. 13). All aged B-TRAF3$^{-/-}$ mice examined (n=4, 9-12 months old), but none of LMC (n=4), had anti-dsDNA autoantibodies in sera (data not shown). Subsequent histopathological examination revealed that 3 out of the 4 aged B-TRAF3$^{-/-}$ mice, but none of the LMC mice, contained lymphocyte infiltrates at multiple locations in kidney and liver (Fig. 7B and data not shown). Furthermore, these 3 aged B-TRAF3$^{-/-}$ mice exhibited immune complex deposition in kidney as evidenced by the co-localized mesangial staining of IgG(H+L) and complement 3 (C3) at glomeruli, which was not detected in any of the LMC mice (Fig. 7C). Thus, specific ablation of TRAF3 in the B cell lineage can be sufficient to induce autoimmune manifestations on the B6 × 129 genetic background.

Discussion

To circumvent the limitations posed by the early lethality of TRAF3$^{-/-}$ mice (Xu et al., 1996), we produced and validated TRAF3$^{flox/flox}$ mice as conditional TRAF3 knockout model systems to allow precise spatial and temporal ablation of TRAF3 expression in the whole animal. This model will be valuable in elucidating the physiological function of TRAF3 in various cell lineages and developmental stages. The initial characterization of this model, described in the present study, revealed a critical role for TRAF3 in inhibiting B cell survival in secondary lymphoid organs and raises the intriguing possibility that TRAF3 is involved in the regulation of self-tolerance.

B-TRAF3$^{-/-}$ mice exhibited B cell expansion from the T2 transitional stage onward, leading to splenomegaly and lymphadenopathy, hypergammaglobulinemia, and autoimmune reactivity, all of which are remarkably similar to the phenotypes of BAFF-transgenic mice and PKCδ$^{-/-}$ mice (Gross et al., 2000; Khare et al., 2000; Mackay et al., 1999; Mecklenbrauker et al., 2004; Mecklenbrauker et al., 2002; Miyamoto et al., 2002). Conversely, BAFF$^{-/-}$, A/WySnJ (carrying a naturally occurring mutation in the BAFF-R gene), BAFF-R$^{-/-}$, and NF-κB2$^{-/-}$ mice display specific B cell loss from the T2 transitional stage onward in peripheral lymphoid organs (Franzoso et al., 1998; Schiemann et al., 2001; Shulga-Morskaya et al., 2004; Thompson et al., 2001). Moreover, TRAF3$^{-/-}$ B cells showed vastly prolonged survival *ex vivo*, markedly increased constitutive activation of NF-κB2 and decreased PKCδ nuclear translocation independent of BAFF. Additional *in vivo* evidence for the elevated constitutive NF-κB2 activity in TRAF3$^{-/-}$ B cells may be the enhanced expression of CD21 and CD23 on splenic and LN B cells in B-TRAF3$^{-/-}$ mice, which mirrors the poor expression of CD21 and CD23 on B cells in BAFF$^{-/-}$ and BAFF-R$^{-/-}$ mice (Schiemann et al., 2001; Shulga-Morskaya et al., 2004). These observations, together with the previous finding that BAFF promotes the expression of CD21 and CD23 (Gorelik et al., 2004), led us to test the hypothesis that TRAF3 functions as a downstream negative regulator of BAFF/BAFF-R signaling. However, *in vivo* administration of TACI-Ig, a potent blocker of BAFF/APRIL signals, failed to deplete

peripheral B cells in B-TRAF3$^{-/-}$ mice. Thus, it is more likely that TRAF3 constitutively inhibits NF-κB2 activation and promotes PKCδ nuclear translocation to induce spontaneous apoptosis in peripheral B cells. In support of this possibility, a previous study provided *in vitro* evidence that TRAF3 constitutively targets NIK, an upstream kinase required for the activation of NF-κB2, for ubiquitination and proteosome-mediated degradation (Liao et al., 2004). Although we could not reproducibly detect NIK protein in TRAF3$^{+/+}$ or TRAF3$^{-/-}$ B cells either in the absence or presence of the proteosome inhibitor MG132 (data not shown), a recent study reported that NIK protein level is increased in TRAF3$^{-/-}$ B cells and MEFs (He et al., 2006), further suggesting that TRAF3 may constitutively target NIK for degradation to inhibit NF-κB2 activation. How TRAF3 constitutively promotes PKCδ nuclear translocation remains to be determined.

In this study, we extended our previous finding obtained with TRAF3$^{-/-}$ B cell lines that CD40-induced NF-κB1, p38 and ERK activation is not affected by TRAF3 deficiency (Xie et al., 2004) to TRAF3$^{-/-}$ splenic B cells. However, CD40-induced JNK activation is increased in TRAF3$^{-/-}$ B cell lines (Xie et al., 2004), but appears to be normal in TRAF3$^{-/-}$ splenic B cells. This difference may be due to the different cellular context of transformed B cell lines *versus* primary splenic B cells. One possibility is that transformed B cell lines may carry mutations in certain genes, whose altered functions may make CD40-induced JNK activation more sensitive to the loss of TRAF3. Another possibility is that because TRAF3$^{-/-}$ splenic B cells developed from pro-B/pre-B/immature B cells in the absence of TRAF3, they may adjust the expression levels of relevant genes (e.g., upregulate the proteins with redundant function, or downregulate the proteins with opposite function) to counteract the deficiency of TRAF3, which might otherwise be detrimental to the development of B cells. Thus, the cell lines may also reflect the effect of TRAF3 deletion only after B cells have completely matured. Taken together, both findings may have physiological relevance: splenic B cells may reflect the situation of altered development in the absence of TRAF3 function, while B cell lines may represent the responses in the case of oncogenic transformation, and/or loss of TRAF3 following complete B cell maturation. In this regard, it should be noted that the expression of TRAF2 is unaltered in TRAF3$^{-/-}$ B cell lines (Xie et al., 2004), but is increased in TRAF3$^{-/-}$ splenic B cells (Fig. 1A). A similar upregulation of TRAF3 expression was observed in TRAF2$^{-/-}$ splenic B cells (Grech et al., 2004). Interestingly, conditional TRAF2$^{-/-}$ mice also display expanded B cell compartments in spleen and LN, and TRAF2$^{-/-}$ B cells also show increased constitutive NF-κB2 activation *ex vivo* (Grech et al., 2004). Thus, TRAF2 and TRAF3 may have redundant function in inhibiting constitutive NF-κB2 activation and B cell survival, and upregulation of either of these TRAF molecules may partially compensate for the loss of the other. Alternatively, TRAF2 and TRAF3 may be redundant positive regulators of constitutive NF-κB2 activation and B cell survival, and the absence of either one may permit the other TRAF to engage the pathway in a way that cannot be normally regulated.

The B lymphocyte is the central player in humoral immunity. Interestingly, we observed that basal serum levels of various Ig isotypes were generally elevated in B-TRAF3$^{-/-}$ mice, with the exception of IgG1 and IgE. Similarly, antibody responses, including IgM and all IgG isotypes, to a T-I Ag were increased in B-TRAF3$^{-/-}$ mice. As antibody responses to TNP-Ficoll are mainly mediated by MZ B cells (Pillai et al., 2005), the increased Ig responses to TNP-Ficoll immunization are consistent with the vastly expanded MZ B cells in these mice. However, in response to the T-D Ag TNP-KLH, although TNP-specific IgM was increased, IgG1 was not increased accordingly. Considering that mature B cells, including follicular and MZ B cells, were markedly expanded in B-TRAF3$^{-/-}$ mice, it is perplexing that these mice displayed neither an increase in the T-D IgG1 response nor an elevation in basal serum IgG1 or IgE levels. It is known that isotype switching to both IgG1 and IgE is regulated by CD40 and IL-4 (Stavnezer and Amemiya, 2004). One possibility is that TRAF3 may participate in this process. As IgG1 is the major antibody produced in T-dependent responses to bacterial

pathogens and soluble protein antigens in mice (Stavnezer and Amemiya, 2004), lack of increase of basal serum IgG1 level may partially reflect the lack of increase in T-dependent IgG1 responses in B-TRAF3$^{-/-}$ mice. Notably, previous studies indicate that CD21 and CD23 play a modulatory role in antibody responses (Haas et al., 2002; Texido et al., 1994; Yu et al., 1994). For example, CD23$^{-/-}$ mice exhibited higher titers of IgG1 and IgE, but normal titers of IgM, IgG2b and IgG3, in response to immunization with T-D Ags (Yu et al., 1994). Consistent with this, transgenic mice overexpressing CD23 on B cells showed reduced IgG1 and IgE serum levels following infection with Nippostrongylus brasiliensis or immunization with anti-IgD Abs (Texido et al., 1994). Thus, it is also possible that the enhanced expression of CD21 and CD23 on B cells may contribute to the serological phenotype of B-TRAF3$^{-/-}$ mice.

Increasing evidence suggests that prolonged survival of B cells contributes to autoimmune diseases (Gauld et al., 2006; Mackay and Kalled, 2002). Peripheral self-tolerance is induced through functional inactivation of autoreactive B cells, termed anergy (Gauld et al., 2006). Prolonged survival of anergic B cells can lead to autoimmunity, simply by providing a greater opportunity for anergic B cells to be recruited to an immune response (Gauld et al., 2006; Mackay and Kalled, 2002). Interestingly, anergic B cells have increased dependence on BAFF for survival, and cannot compete with normal B cells for a limiting source of BAFF (Gauld et al., 2006; Lesley et al., 2004). Thus, the prolonged BAFF-independent survival capacity of TRAF3$^{-/-}$ B cells may predispose B-TRAF3$^{-/-}$ mice to develop autoimmune reactivity. Indeed, the majority of B-TRAF3$^{-/-}$ mice already exhibited numerous and large spontaneous splenic GCs in the absence of immunization, and developed anti-dsDNA autoantibodies in the serum by the age of 10-12 weeks. Furthermore, aged B-TRAF3$^{-/-}$ mice developed additional autoimmune manifestations, including lymphocyte infiltration in kidney and liver, and immune complex deposition in kidney. Thus, specific deletion of TRAF3 in B cells appears to be sufficient to induce autoimmune alterations in mice. However, it should be noted that B-TRAF3$^{-/-}$ mice had a mixed genetic background of B6 × 129, and that epistatic interactions between the B6 and 129 genomes have important impacts on systemic autoimmune manifestations (Manderson et al., 2004; Wakeland et al., 2001). For example, C1q deficiency is associated with anti-nuclear antibody production and glomerulonephritis in B6 × 129 hybrid mice, but not in either parental strain (Manderson et al., 2004). Similarly, bcl-2 transgenic expression in B cells leads to immune complex glomerulonephritis in B6 × SJL hybrid mice, but not on a B6 × C3H genetic background (McDonnell et al., 1989; Strasser et al., 1991). Thus, the mixed genetic background of B6 × 129 may contribute to the serological variations observed in B-TRAF3$^{-/-}$ mice, and may make the mice more sensitive to the loss of TRAF3 and prone to autoimmune alterations. Nevertheless, our results indicate that TRAF3 deficiency can be a predisposing genetic factor to autoimmune diseases in mice.

Extended lifespan of B cells and B cell hyperplasia have been associated with B leukemiagenesis and B lymphomagenesis (Cory et al., 2003; Mackay and Tangye, 2004; Packham and Stevenson, 2005). Whether B-TRAF3$^{-/-}$ mice have increased propensity to develop lymphomas awaits investigation. Nonetheless, prolonged survival of TRAF3$^{-/-}$ B cells could predispose them to transformation in response to additional oncogenic events, such as viral infections, chronic inflammation, mutations or chromosomal translocations involving oncogenes or tumor suppressor genes. Consistent with this, elevated serum BAFF has been detected in humans with autoimmune diseases as well as B cell malignancies (Mackay and Tangye, 2004). Constitutively activated mutant forms of NF-κB2, caused by chromosomal translocations, have also been detected in patients with B lymphomas (Karin et al., 2002). It would thus be interesting to investigate whether inactivating mutations of the TRAF3 gene or decreased expression of TRAF3 occur in human patients with autoimmune diseases as well as B leukemias and lymphomas. The new mouse model presented here suggests that specifically enhancing TRAF3 activity or expression in B cells may be of therapeutic value in combating these human diseases.

Experimental procedures

Generation of conditional TRAF3$^{-/-}$ mice

TRAF3$^{+/flox}$ mice were generated using standard protocols as detailed in the Supplementary experimental procedures, and were interbred to generate TRAF3$^{flox/flox}$ mice. TRAF3$^{flox/flox}$ mice were crossed with CD19$^{Cre/Cre}$ mice (Rickert et al., 1997)(Jackson Laboratory) to generate TRAF3$^{+/flox}$CD19$^{+/Cre}$ mice, which were subsequently backcrossed with TRAF3$^{flox/flox}$ mice to generate TRAF3$^{flox/flox}$CD19$^{+/Cre}$ (B-TRAF3$^{-/-}$) mice. Deletion of exons 1 and 2 of the TRAF3 gene in splenic B cells was detected by genomic PCR using primers U7 and BT6 (Supplementary Fig. 1C). B-TRAF3$^{-/-}$ mice analyzed had a mixed genetic background between 129/SvJ and C57BL/6, and littermates were used as controls for all experiments. All mice were kept in specific pathogen-free conditions in the Gene Targeting Core Facility at the University of Iowa, and were used in accordance with NIH guidelines and under an animal protocol approved by the Animal Care and Use Committee of the University of Iowa.

Primers, antibodies, reagents and methods for supplementary figures

Details of primers, Abs, reagents, and methods for supplementary figures are described in the Supplementary experimental procedures.

Flow cytometry

Single cell suspensions were made from the spleen, LN, thymus, BM and peritoneal lavages. Erythrocytes from spleen were depleted with ACK lysis buffer. Cells (0.5×10^6) were then blocked with rat serum and FcR blocking Ab (2.4G2), and incubated with various Abs conjugated to FITC, PE, PerCP, or Cy5 for multiple color fluorescence surface staining. For cellularity analysis, cell surface markers examined include CD45R (B220), CD3, AA4.1, c-Kit, CD25, CD1d, CD9, CD19, CD21, CD23, CD5, IgM, IgD, CD38, CD43, CD4, CD8, CD11b, Gr-1, and MHC class II (I-A/I-E) as indicated in the Figures and Supplementary Table 1. Listmode data were acquired on a FACSVantage (Becton Dickinson, Mountain View, CA) using Cell Quest software. The results were analyzed using FlowJo software (TreeStar, San Carlos, CA). FSC/SSC gating for single lymphocytes, which exclude cell aggregates, small erythrocytes and dead cell debris, was used to analyze flow cytometric data.

Hematoxylin-eosin staining of tissues

Mouse LN, kidney and liver were fixed in 10% neutral formalin, then processed and embedded in paraffin. Microsections (5 μm) of paraffin blocks were prepared using a microtome (HM 355, Microm, Walldorf, Germany), and were stained with hematoxylin and eosin using an automated slide stainer (Sakura DRS 601 Diversified Stainer, Sakura). Stained slides were mounted with Solvent 100 mounting media, and bright field micrographs of stained sections were taken using a microscope (Olympus BX-51, Olympus America Inc., Center Valley, PA) fitted with an Olympus DP70 camera (Olympus America Inc.).

Immunohistochemistry

Spleens were harvested from naïve mice or mice immunized i.p. with 0.1 ml of 10% SRBC in PBS for 10 days. Kidneys were collected from aged naïve mice. Tissues were soaked in 20% sucrose in PBS for 20 min, embedded with OCT compound and snap-frozen in liquid N2. Frozen sections (8-10 μm) were prepared using a cryostat (HM505E, Microm), and fixed with cold acetone. Rehydration, blocking and staining of sections were carried out as described (Stunz et al., 2004). Spleen sections were stained with FITC-PNA, Alexa Fluor 350-anti-mouse IgM Ab, and PE-anti-mouse CD3 Ab to determine splenic architecture, or with FITC-anti-mouse MOMA-1 Ab and PE-B220 to visualize MZ B cells. Kidney sections were stained with

FITC-anti-mouse C3 Ab and PE-anti-mouse IgG (H+L) Ab. Stained slides were mounted with VectorShield, and observed on a fluorescence microscope (Olympus BX-60, Olympus America Inc.) fitted with a Sensys camera (Photometrics, Tucson, AZ). Images were analyzed by using ImagePro4.5 software (Media Cybernetics, Silver Spring, MD).

Immunizations and ELISAs

Basal serum levels of various Ig isotypes were analyzed by ELISA as previously described (Stunz et al., 2004). In the IgE-specific ELISA, capture mAb was EM95, and detection Ab was Alkaline phosphatase (AP)-conjugated goat anti-mouse IgE Ab. All the other capture Abs and AP-conjugated detection Abs were polyclonal goat Abs, including Abs specific for mouse IgM, IgG1, IgG2a, IgG2b, IgG3, and IgA. Plates were read on a Versamax plate reader (Molecular Devices, Sunnyvale, CA) and results analyzed by using SoftMax Pro 4.0 software. Standard curves were included on each plate by using purified standards (Southern Biotechnology Associates) for each Ig isotype. For T-I antibody responses, mice were immunized i.p. with 50 μg of TNP-Ficoll (Biosource Technologies, Vacaville, CA) precipitated in alum. Sera were collected on day 10 after immunization. TNP-specific Abs in sera were measured with the use of ELISA plates coated with TNP_{38}-conjugated bovine serum albumin. Bound Abs were detected with AP-conjugated goat anti-mouse IgM, IgG1, IgG2a, IgG2b, or IgG3 Abs, respectively. For T-D antibody responses, mice were immunized i.p. with 100 μg of TNP-KLH (Biosource Technologies) precipitated in alum, and boosted with 100 μg of TNP-KLH/alum on day 21. Sera were collected on day 7, 14 and 28 after the first immunization. Serum levels of anti-TNP IgM and IgG1 were measured by ELISA as described above. For TNP-specific IgG1 or IgG2a, standard curves were determined on each plate using serial dilutions of purified standards (BD Pharmingen). For TNP-specific IgM, IgG2b or IgG3, standard curves were determined on each plate using serial dilutions of a standard serum. Multiple 1:5 or 1:10 serial dilutions of each serum sample were examined in each TNP-specific Ig isotype ELISA, and the range of the dilution factors tested is from 1:100 to 1:1000000. Each standard curve contained 11 dilution points, and in all cases, the coefficiency of determination for the standard curve (r2) was >0.98. The dilution factor that gave A405 (O.D.405nm) values within the linear range (0.1 ~ 1.5) of standard curves of ELISA was used to calculate the concentrations of TNP-specific IgG1 and IgG2a, or relative titers of TNP-specific IgM, IgG2b and IgG3. Relative titers were calculated according to the formula: Relative titer = A405 value × 10 × dilution factor, and therefore reflect the relative concentrations of each TNP-specific Ig isotype in arbitrary units.

Splenic B cell purification

Splenic B cells and non-B cells were separated using anti-mouse CD43-coated magnetic beads and a MACS separator (Miltenyi Biotec Inc.) following the manufacturer's protocols. For purification of resting splenic B cells, high density resting splenocytes were first isolated by density gradient centrifugation through a 60:65:85% Percoll gradient. Resting lymphocytes at the interface between 65% and 85% Percoll were collected, and resting B cells were further purified by negative selection using anti-mouse CD43 magnetic beads according to the manufacturer's protocols. The purity of isolated populations was monitored by FACS analysis using Cy5-anti-B220, FITC-anti-IgM and PE-anti-Fas, and cell preparations of >90% purity were used for further experiments. Purified resting splenic B cells were cultured in mouse culture medium (RPMI 1640 medium supplemented with 5% FCS, 10 μM β-mercaptoethanol, 10 mM Hepes (pH 7.55), 1 mM sodium pyruvate, 2 mM L-glutamine, and 0.1 mM non-essential amino acids).

Survival assay and cell cycle analysis

Purified resting splenic B cells ($0.5X10^6$/ml/well) were cultured in 24-well plates in the absence or presence of 0.5 μg/ml BAFF, or 2 μg/ml of anti-mouse CD40 Ab (HM40-3) at 37°C. Cells were fed with fresh medium containing the appropriate stimulation every 4 days. At each time point, cells was taken to determine the number of viable cells by staining with Trypan blue. For PI staining, cells were fixed with an equal volume of ice-cold 70% ethanol. PI staining was performed as previously described (Catlett et al., 2001), and DNA content was quantified by a benchtop FACScan (Becton Dickinson). Labeling of B cells with CFSE (Molecular Probes) for proliferation analysis was performed following the manufacturer's instructions. Labeled cells were cultured in the absence or presence of 2 μg/ml of anti-mouse CD40 Ab (HM40-3), alone or in combination with 10 μg/ml of anti-mouse IgM (Fab') or 100 ng/ml of IL-4 at 37° C for 4 days. Cells were then fixed, and the decline in CFSE fluorescence as a measure of proliferation was determined by FACS analysis.

Immunoblot analysis

For detection of TRAF3 expression in B cells versus non-B cells, purified CD43+ and CD43- splenocytes were directly lysed as previously described (Xie and Bishop, 2004). For detection of the activation of NF-κB1 or MAP kinases, purified resting splenic B cells were cultured in the absence or presence of 2 μg/ml of anti-mouse CD40 Ab (HM40-3) at 37°C for various time periods as indicated in the Figures, and total cellular lysates were prepared. For detection of nuclear translocation of NF-κB2 and PKCδ, purified resting splenic B cells were cultured in the absence or presence of 0.5 μg/ml BAFF, or 2 μg/ml of anti-mouse CD40 Ab (HM40-3) at 37°C for 24 h. Cytosolic and nuclear extracts were prepared as described (Xie et al., 2006). Immunoblot analysis was performed using various antibodies as previously described (Xie and Bishop, 2004). Bands of immunoblots were quantitated using a low-light imaging system (LAS-1000, FUJIFILM Medical Systems USA, Inc., Stamford, CT).

In vivo administration of TACI-Ig

Mice (10 weeks old) were injected i.p. with 100 μg of TACI-Ig (R&Dsystems, Minneapolis, MN) or a control Ig (human Ig Fc), three times/week for 15 days.

Detection of anti-dsDNA autoantibodies

Sera from naive mice were tested for autoantibodies using ELISA kits detecting anti-dsDNA Abs (Alpha Diagnostic, San Antonio, TX) following the manufacturer's protocols. Standards, negative and positive control sera provided by the manufacturer were run concurrently with the unknown samples. The specificity of anti-dsDNA autoantibodies detected in B-TRAF3$^{-/-}$ mice was verified by a second assay using *Crithidia luciliae* dsDNA substrate slides (The Binding Site, Birmingham, UK) as previously described (Stunz et al., 2004).

Statistics

For direct comparison of spontaneous GC B cells and Ig isotype levels of LMC and B-TRAF3$^{-/-}$ mice, statistical significance was determined with the unpaired *t* test for two-tailed data. *P* values less than 0.05 are considered significant, and *P* values less than 0.01 are considered very significant.

Supplementary Material

Refer to Web version on PubMed Central for supplementary material.

Acknowledgements

This study was supported by a National Scientist Development grant from the American Heart Association (P. Xie), and National Institutes of Health grants AI28847, AI49993, CA099997, and a VA Career Award (G. Bishop). We are grateful to Dr. Thomas Waldschmidt for his expert advice on FACS data analysis, and Dr. David Meyerholz for pathological evaluation of HE- and immunofluorescence-stained tissue sections. We would like to thank Thomas Kinney for expert animal husbandry, Kyp Oxley for excellent technical assistance, Kathy Walters and Chantal Allamargot of the Central Microscopy Research Facility for technical help in microsection and HE staining, and Drs. Jon Houtman and Bruce Hostager for stimulating discussions and critical review of the manuscript.

References

Bishop GA. The multifaceted roles of TRAFs in the regulation of B-cell function. Nat. Rev. Immunol 2004;4:775–786. [PubMed: 15459669]

Catlett IM, Xie P, Hostager BS, Bishop GA. Signaling through MHC class II molecules blocks CD95-induced apoptosis. J. Immunol 2001;166:6019–6024. [PubMed: 11342618]

Claudio E, Brown K, Park S, Wang H, Siebenlist U. BAFF-induced NEMO-independent processing of NF-kappa B2 in maturing B cells. Nat. Immunol 2002;3:958–965. [PubMed: 12352969]

Cory S, Huang DC, Adams JM. The Bcl-2 family: roles in cell survival and oncogenesis. Oncogene 2003;22:8590–8607. [PubMed: 14634621]

Franzoso G, Carlson L, Poljak L, Shores EW, Epstein S, Leonardi A, Grinberg A, Tran T, Scharton-Kersten T, Anver M, et al. Mice deficient in nuclear factor (NF)-kappa B/p52 present with defects in humoral responses, germinal center reactions, and splenic microarchitecture. J. Exp. Med 1998;187:147–159. [PubMed: 9432973]

Gauld SB, Merrell KT, Cambier JC. Silencing of autoreactive B cells by anergy: a fresh perspective. Curr. Opin. Immunol 2006;18:292–297. [PubMed: 16616480]

Gorelik L, Cutler AH, Thill G, Miklasz SD, Shea DE, Ambrose C, Bixler SA, Su L, Scott ML, Kalled SL. Cutting edge: BAFF regulates CD21/35 and CD23 expression independent of its B cell survival function. J. Immunol 2004;172:762–766. [PubMed: 14707045]

Grammer AC, Lipsky PE. CD40-mediated regulation of immune responses by TRAF-dependent and TRAF-independent signaling mechanisms. Adv. Immunol 2000;76:61–178. [PubMed: 11079098]

Grech AP, Amesbury M, Chan T, Gardam S, Basten A, Brink R. TRAF2 differentially regulates the canonical and noncanonical pathways of NF-kappaB activation in mature B cells. Immunity 2004;21:629–642. [PubMed: 15539150]

Gross JA, Dillon SR, Mudri S, Johnston J, Littau A, Roque R, Rixon M, Schou O, Foley KP, Haugen H, et al. TACI-Ig neutralizes molecules critical for B cell development and autoimmune disease. impaired B cell maturation in mice lacking BLyS. Immunity 2001;15:289–302. [PubMed: 11520463]

Gross JA, Johnston J, Mudri S, Enselman R, Dillon SR, Madden K, Xu W, Parrish-Novak J, Foster D, Lofton-Day C, et al. TACI and BCMA are receptors for a TNF homologue implicated in B-cell autoimmune disease. Nature 2000;404:995–999. [PubMed: 10801128]

Haas KM, Hasegawa M, Steeber DA, Poe JC, Zabel MD, Bock CB, Karp DR, Briles DE, Weis JH, Tedder TF. Complement receptors CD21/35 link innate and protective immunity during Streptococcus pneumoniae infection by regulating IgG3 antibody responses. Immunity 2002;17:713–723. [PubMed: 12479818]

Hacker H, Redecke V, Blagoev B, Kratchmarova I, Hsu LC, Wang GG, Kamps MP, Raz E, Wagner H, Hacker G, et al. Specificity in Toll-like receptor signalling through distinct effector functions of TRAF3 and TRAF6. Nature 2006;439:204–207. [PubMed: 16306937]

He JQ, Zarnegar B, Oganesyan G, Saha SK, Yamazaki S, Doyle SE, Dempsey PW, Cheng G. Rescue of TRAF3-null mice by p100 NF-kappa B deficiency. J. Exp. Med 2006;203:2413–2418. [PubMed: 17015635]

Karin M, Cao Y, Greten FR, Li ZW. NF-kappaB in cancer: from innocent bystander to major culprit. Nat. Rev. Cancer 2002;2:301–310. [PubMed: 12001991]

Khare SD, Sarosi I, Xia XZ, McCabe S, Miner K, Solovyev I, Hawkins N, Kelley M, Chang D, Van G, et al. Severe B cell hyperplasia and autoimmune disease in TALL-1 transgenic mice. Proc. Natl. Acad. Sci. U S A 2000;97:3370–3375. [PubMed: 10716715]

Lesley R, Xu Y, Kalled SL, Hess DM, Schwab SR, Shu HB, Cyster JG. Reduced competitiveness of autoantigen-engaged B cells due to increased dependence on BAFF. Immunity 2004;20:441–453. [PubMed: 15084273]

Liao G, Zhang M, Harhaj EW, Sun SC. Regulation of the NF-kappaB-inducing kinase by tumor necrosis factor receptor-associated factor 3-induced degradation. J. Biol. Chem 2004;279:26243–26250. [PubMed: 15084608]

Mackay F, Kalled SL. TNF ligands and receptors in autoimmunity: an update. Curr. Opin. Immunol 2002;14:783–790. [PubMed: 12413530]

Mackay F, Schneider P, Rennert P, Browning J. BAFF AND APRIL: a tutorial on B cell survival. Annu. Rev. Immunol 2003;21:231–264. [PubMed: 12427767]

Mackay F, Tangye SG. The role of the BAFF/APRIL system in B cell homeostasis and lymphoid cancers. Curr. Opin. Pharmacol 2004;4:347–354. [PubMed: 15251127]

Mackay F, Woodcock SA, Lawton P, Ambrose C, Baetscher M, Schneider P, Tschopp J, Browning JL. Mice transgenic for BAFF develop lymphocytic disorders along with autoimmune manifestations. J. Exp. Med 1999;190:1697–1710. [PubMed: 10587360]

Manderson AP, Botto M, Walport MJ. The role of complement in the development of systemic lupus erythematosus. Annu. Rev. Immunol 2004;22:431–456. [PubMed: 15032584]

McDonnell TJ, Deane N, Platt FM, Nunez G, Jaeger U, McKearn JP, Korsmeyer SJ. bcl-2-immunoglobulin transgenic mice demonstrate extended B cell survival and follicular lymphoproliferation. Cell 1989;57:79–88. [PubMed: 2649247]

Mecklenbrauker I, Kalled SL, Leitges M, Mackay F, Tarakhovsky A. Regulation of B-cell survival by BAFF-dependent PKCdelta-mediated nuclear signalling. Nature 2004;431:456–461. [PubMed: 15361883]

Mecklenbrauker I, Saijo K, Zheng NY, Leitges M, Tarakhovsky A. Protein kinase Cdelta controls self-antigen-induced B-cell tolerance. Nature 2002;416:860–865. [PubMed: 11976686]

Miller JP, Stadanlick JE, Cancro MP. Space, selection, and surveillance: setting boundaries with BLyS. J. Immunol 2006;176:6405–6410. [PubMed: 16709796]

Miyamoto A, Nakayama K, Imaki H, Hirose S, Jiang Y, Abe M, Tsukiyama T, Nagahama H, Ohno S, Hatakeyama S, Nakayama KI. Increased proliferation of B cells and auto-immunity in mice lacking protein kinase Cdelta. Nature 2002;416:865–869. [PubMed: 11976687]

Morrison MD, Reiley W, Zhang M, Sun SC. An atypical tumor necrosis factor (TNF) receptor-associated factor-binding motif of B cell-activating factor belonging to the TNF family (BAFF) receptor mediates induction of the noncanonical NF-kappaB signaling pathway. J. Biol. Chem 2005;280:10018–10024. [PubMed: 15644327]

Oganesyan G, Saha SK, Guo B, He JQ, Shahangian A, Zarnegar B, Perry A, Cheng G. Critical role of TRAF3 in the Toll-like receptor-dependent and - independent antiviral response. Nature 2006;439:208–211. [PubMed: 16306936]

Packham G, Stevenson FK. Bodyguards and assassins: Bcl-2 family proteins and apoptosis control in chronic lymphocytic leukaemia. Immunology 2005;114:441–449. [PubMed: 15804279]

Pasparakis M, Schmidt-Supprian M, Rajewsky K. IkappaB kinase signaling is essential for maintenance of mature B cells. J. Exp. Med 2002;196:743–752. [PubMed: 12235208]

Pillai S, Cariappa A, Moran ST. Marginal zone B cells. Annu. Rev. Immunol 2005;23:161–196. [PubMed: 15771569]

Quezada SA, Jarvinen LZ, Lind EF, Noelle RJ. CD40/CD154 interactions at the interface of tolerance and immunity. Annu. Rev. Immunol 2004;22:307–328. [PubMed: 15032580]

Rickert RC, Roes J, Rajewsky K. B lymphocyte-specific, Cre-mediated mutagenesis in mice. Nucleic Acids Res 1997;25:1317–1318. [PubMed: 9092650]

Sasaki Y, Derudder E, Hobeika E, Pelanda R, Reth M, Rajewsky K, Schmidt-Supprian M. Canonical NF-kappaB activity, dispensable for B cell development, replaces BAFF-receptor signals and promotes B cell proliferation upon activation. Immunity 2006;24:729–739. [PubMed: 16782029]

Schiemann B, Gommerman JL, Vora K, Cachero TG, Shulga-Morskaya S, Dobles M, Frew E, Scott ML. An essential role for BAFF in the normal development of B cells through a BCMA-independent pathway. Science 2001;293:2111–2114. [PubMed: 11509691]

Shulga-Morskaya S, Dobles M, Walsh ME, Ng LG, MacKay F, Rao SP, Kalled SL, Scott ML. B Cell-Activating Factor Belonging to the TNF Family Acts through Separate Receptors to Support B Cell Survival and T Cell-Independent Antibody Formation. J. Immunol 2004;173:2331–2341. [PubMed: 15294946]

Stavnezer J, Amemiya CT. Evolution of isotype switching. Semin. Immunol 2004;16:257–275. [PubMed: 15522624]

Strasser A, Whittingham S, Vaux DL, Bath ML, Adams JM, Cory S, Harris AW. Enforced BCL2 expression in B-lymphoid cells prolongs antibody responses and elicits autoimmune disease. Proc. Natl. Acad. Sci. U S A 1991;88:8661–8665. [PubMed: 1924327]

Stunz LL, Busch LK, Munroe ME, Sigmund CD, Tygrett LT, Waldschmidt TJ, Bishop GA. Expression of the Cytoplasmic Tail of LMP1 in Mice Induces Hyperactivation of B Lymphocytes and Disordered Lymphoid Architecture. Immunity 2004;21:255–266. [PubMed: 15308105]

Texido G, Eibel H, Le Gros G, van der Putten H. Transgene CD23 expression on lymphoid cells modulates IgE and IgG1 responses. J. Immunol 1994;153:3028–3042. [PubMed: 8089484]

Thompson JS, Bixler SA, Qian F, Vora K, Scott ML, Cachero TG, Hession C, Schneider P, Sizing ID, Mullen C, et al. BAFF-R, a newly identified TNF receptor that specifically interacts with BAFF. Science 2001;293:2108–2111. [PubMed: 11509692]

Wajant H, Henkler F, Scheurich P. The TNF-receptor-associated factor family. Scaffold molecules for cytokine receptors, kinases and their regulators. Cell Signal 2001;13:389–400. [PubMed: 11384837]

Wakeland EK, Liu K, Graham RR, Behrens TW. Delineating the genetic basis of systemic lupus erythematosus. Immunity 2001;15:397–408. [PubMed: 11567630]

Xie P, Bishop GA. Roles of TNF receptor-associated factor 3 in signaling to B lymphocytes by carboxyl-terminal activating regions 1 and 2 of the EBV-encoded oncoprotein latent membrane protein 1. J. Immunol 2004;173:5546–5555. [PubMed: 15494504]

Xie P, Hostager BS, Bishop GA. Requirement for TRAF3 in Signaling by LMP1 But Not CD40 in B Lymphocytes. J. Exp. Med 2004;199:661–671. [PubMed: 14981114]

Xie P, Hostager BS, Munroe ME, Moore CR, Bishop GA. Cooperation between TNF receptor-associated factors 1 and 2 in CD40 signaling. J. Immunol 2006;176:5388–5400. [PubMed: 16622006]

Xu Y, Cheng G, Baltimore D. Targeted disruption of TRAF3 leads to postnatal lethality and defective T-dependent immune responses. Immunity 1996;5:407–415. [PubMed: 8934568]

Yu P, Kosco-Vilbois M, Richards M, Kohler G, Lamers MC. Negative feedback regulation of IgE synthesis by murine CD23. Nature 1994;369:753–756. [PubMed: 8008068]

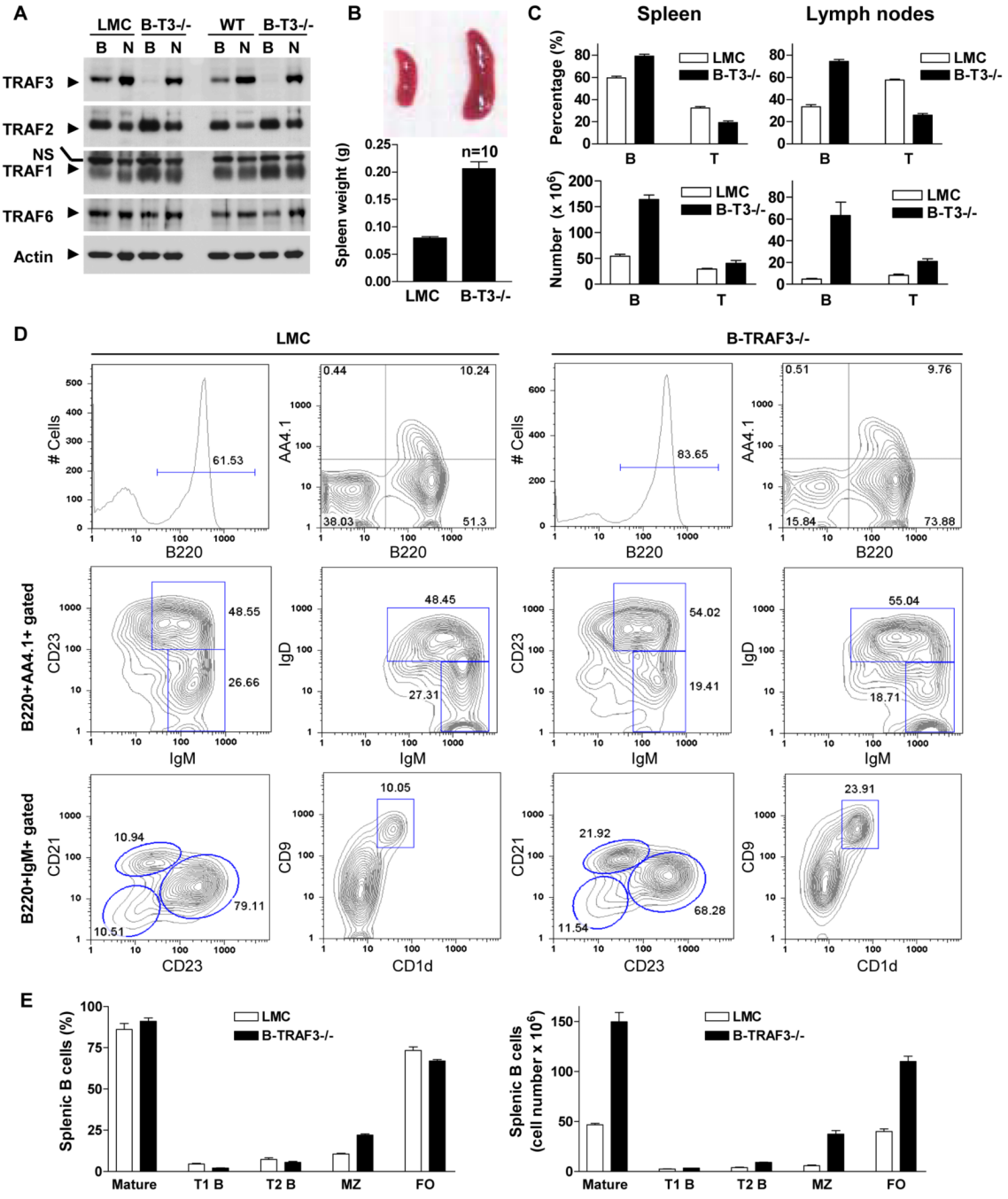

Figure 1. Expanded B cell compartments in spleens and lymph nodes of B-TRAF3$^{-/-}$ mice

(**A**) Verification of TRAF3 deletion in B cells by Western blot analysis. Splenic B cells were purified from LMC and B-TRAF3$^{-/-}$ (B-T3-/-) mice by negative selection using CD43-magnetic beads. Total cellular proteins were extracted from both the purified B cells (B) and the CD43+ (mainly non-B) cells (N). The same protein blot was first immunoblotted for TRAF3, then stripped and re-probed for TRAF2, TRAF1, TRAF6, and actin. NS, non-specific band. Results shown are representative of 3 independent experiments. (**B**) Enlarged spleen of B-TRAF3$^{-/-}$ mice. Top panel shows photo of representative spleens of LMC and B-TRAF3$^{-/-}$ mice, and bottom panel depicts spleen weights (mean ± SEM, n=10 for each group of mice). (**C**) Percentages and numbers of B and T cells in spleens and LN of LMC and B-TRAF3$^{-/-}$

mice. B cells and T cells were identified by FACS analysis using markers described in Supplementary Table 1. The graph depicts the results of four independent experiments (mean ± SEM). (**D**) Representative FACS histograms or contour plots of splenic B cells of LMC and B-TRAF3$^{-/-}$ mice. FACS profiles were scatter-gated on single lymphocytes. T1, T2, follicular (FO), and marginal zone (MZ) B cell populations were identified using markers described in Supplementary Table 1. Similar results were observed in three additional experiments. (**E**) Percentages (among total B cells) and numbers of splenic B cell subsets of LMC and B-TRAF3$^{-/-}$ mice. The graph depicts the results of four independent experiments (mean ± SEM). Mice analyzed were 8 to 12 weeks old.

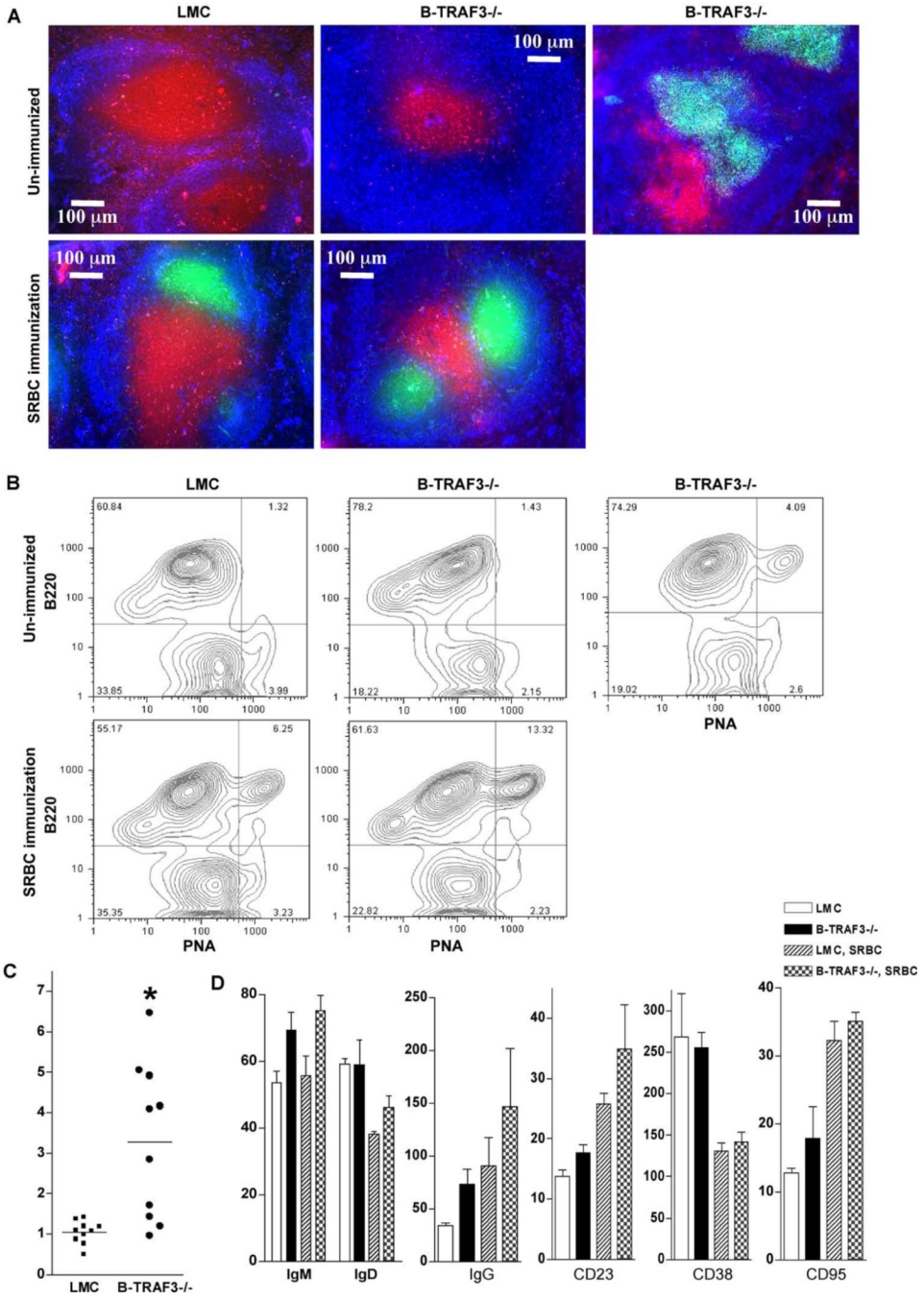

Figure 2. Spontaneous germinal centers in B-TRAF3$^{-/-}$ mice

(**A**) Splenic architecture of LMC and B-TRAF3$^{-/-}$ mice. Frozen sections were prepared from spleens of naïve mice or mice immunized with SRBC at 11 days post-immunization, and stained with PNA-FITC (green), anti-IgM-Alexa Fluor 350 (blue), and anti-CD3-PE (red). (**B**) GC B cells analyzed by FACS analysis. Representative FACS contour plots of splenocytes of LMC and B-TRAF3$^{-/-}$ mice are shown. Similar results were observed in two additional experiments. (**C**) Percentage of spontaneous GC B cells (B220+PNA+) of LMC and B-TRAF3$^{-/-}$ mice (n=10 for each group of mice). *, very significantly different from LMC (*t*-test, $P<0.005$). (**D**) Distinct expression profile of GC B cells of B-TRAF3$^{-/-}$ mice. Splenocytes of naïve mice or mice immunized with SRBC at 11 days post-immunization were analyzed by

FACS staining. The graph depicts the mean channel fluorescence (MCF) of IgM, IgD, IgG, CD23, CD38 and CD95 expression on B220+PNA+-gated splenocytes. Data shown are the results of three independent experiments (mean ± SEM). Mice analyzed were 10 to 12 weeks old.

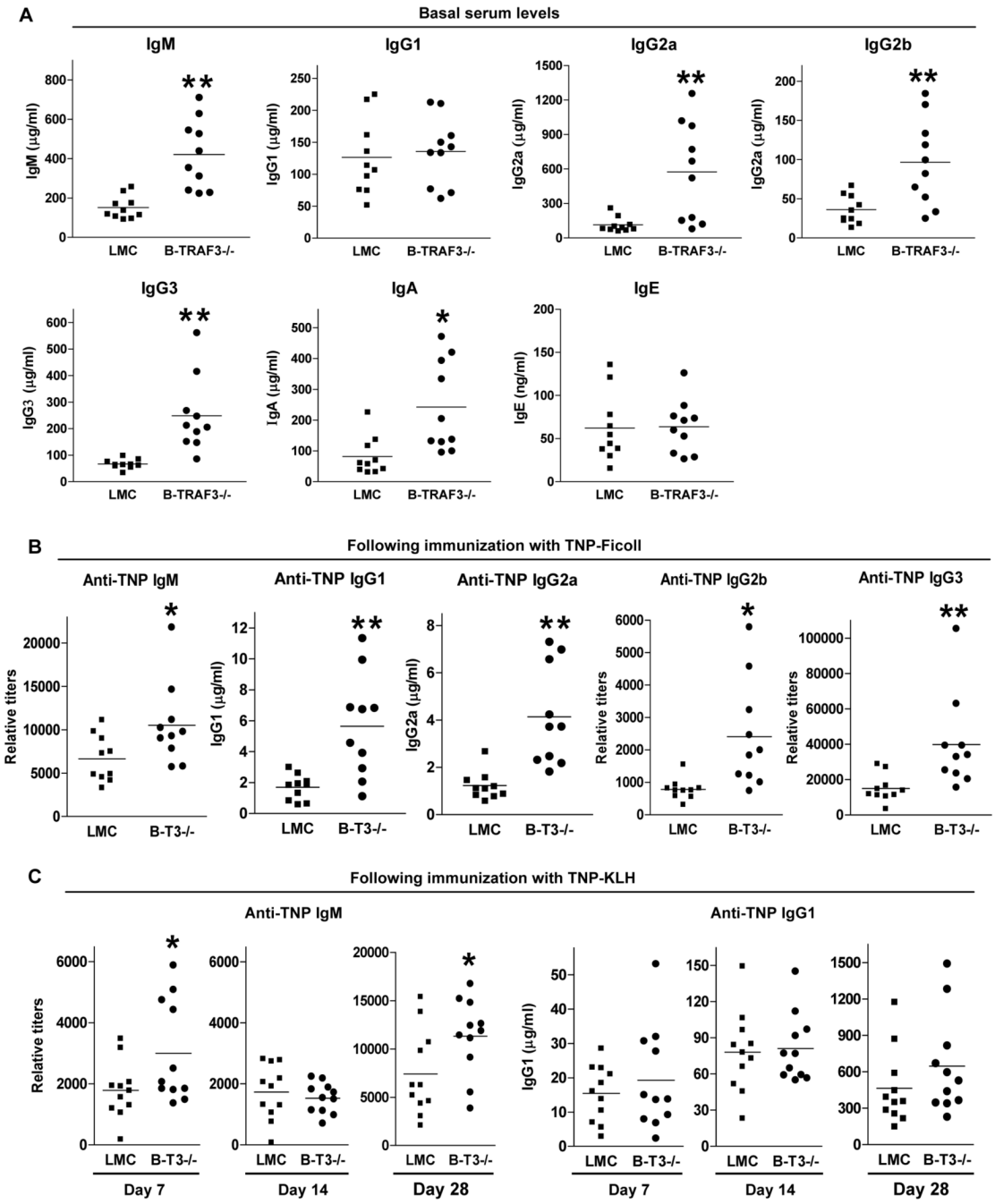

Figure 3. Altered antibody responses in B-TRAF3$^{-/-}$ mice

(**A**) Basal serum levels of Ig isotypes. Sera from naïve LMC and B-TRAF3$^{-/-}$ mice (n=10 for each group) were tested for IgM, IgG1, IgG2a, IgG2b, IgG3, and IgE by ELISA. Mice analyzed were 10 to 12 weeks old. (**B**) T-I antibody responses. Mice (8-10 weeks old, n=10 for each group) were immunized with the T-I Ag TNP-Ficoll/Alum, and sera were collected on day 10 after immunization. Serum levels of anti-TNP IgM, IgG1, IgG2a, IgG2b and IgG3 were analyzed by ELISA. (**C**) T-D antibody responses. Mice (8-10 weeks old, n=11 for each group) were immunized with the T-D Ag TNP-KLH/Alum, and boosted on day 21 after the first immunization. Sera were collected on day 7, 14 and 28 after the first immunization. Serum levels of anti-TNP IgM and IgG1 were measured by ELISA. Multiple serial dilutions of each

serum sample were tested to ensure the readout is within the linear range of the assay. Relative titer = A405 value × 10 × Dilution factor. Anti-TNP specific Ig levels in pre-immune sera (with 1:100 dilution) of both littermate control and B-TRAF3$^{-/-}$ mice were below the detection limit of ELISA. *, significantly different from LMC (*t*-test, $P<0.05$); **, very significantly different from LMC (*t*-test, $P<0.01$).

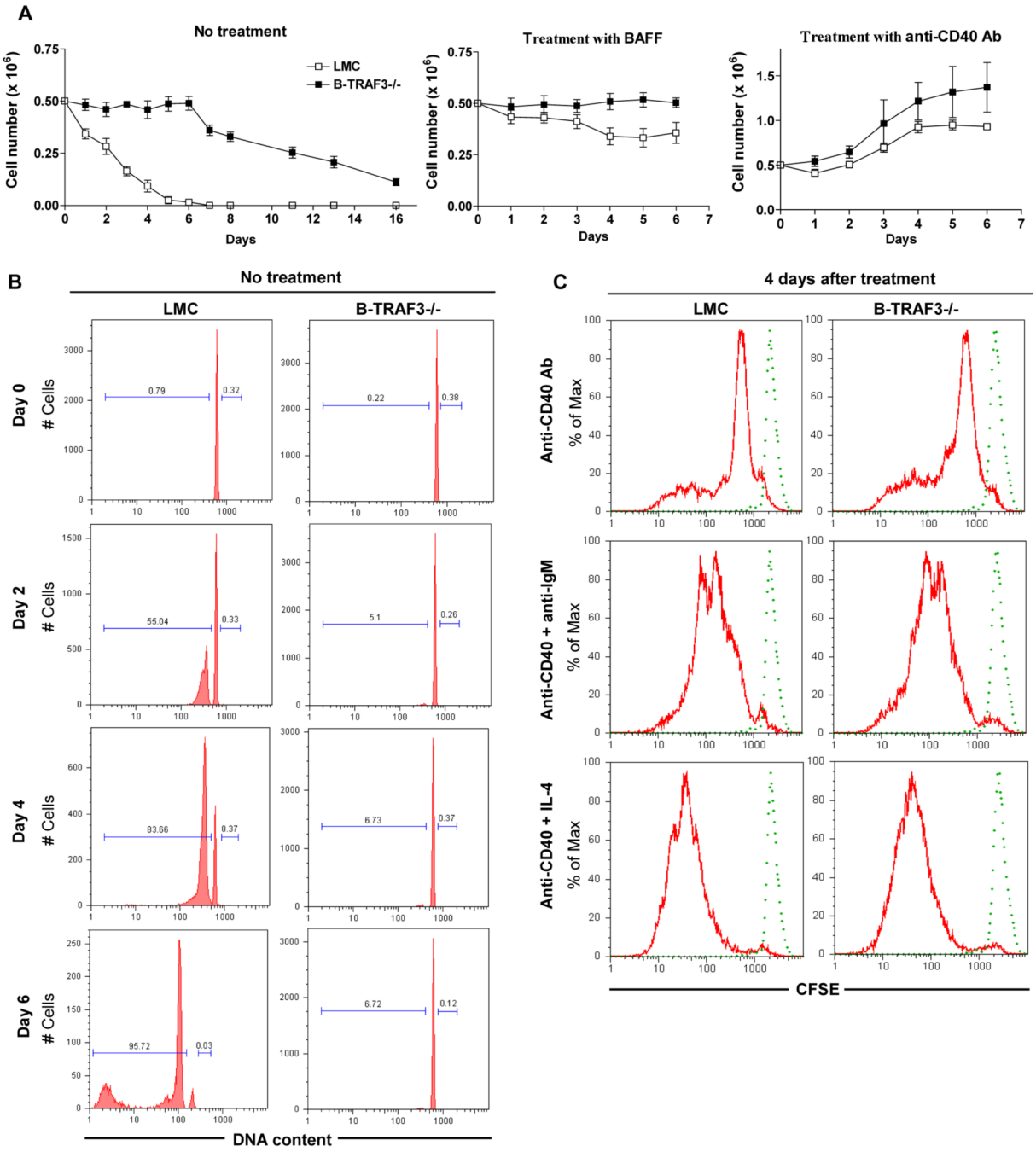

Figure 4. Prolonged survival of TRAF3$^{-/-}$ resting splenic B cells ex vivo

Resting splenic B cells were purified from 8- to 12- week-old LMC and B-TRAF3$^{-/-}$ mice, and cultured in the absence or presence of stimulation as indicated. (**A**) B cell survival *ex vivo*. The numbers of viable cells at each time point were determined by staining with Trypan blue. Data shown are results of three independent experiments (mean ± SEM). (**B**) Cell cycle analysis by PI staining and FACS. Representative histograms of PI staining are shown, and percentage of apoptotic cells (DNA content < 2n) and proliferating cells (2n < DNA content ≤ 4n) are indicated. (**C**) B cell proliferation analyzed by CFSE-labeling. Dashed FACS profile shows CFSE signals of freshly labeled cells, while solid profile shows diluted CFSE signals of cells

cultured ex vivo for 4 days in the presence of indicated stimulation. Similar results were observed in two additional experiments.

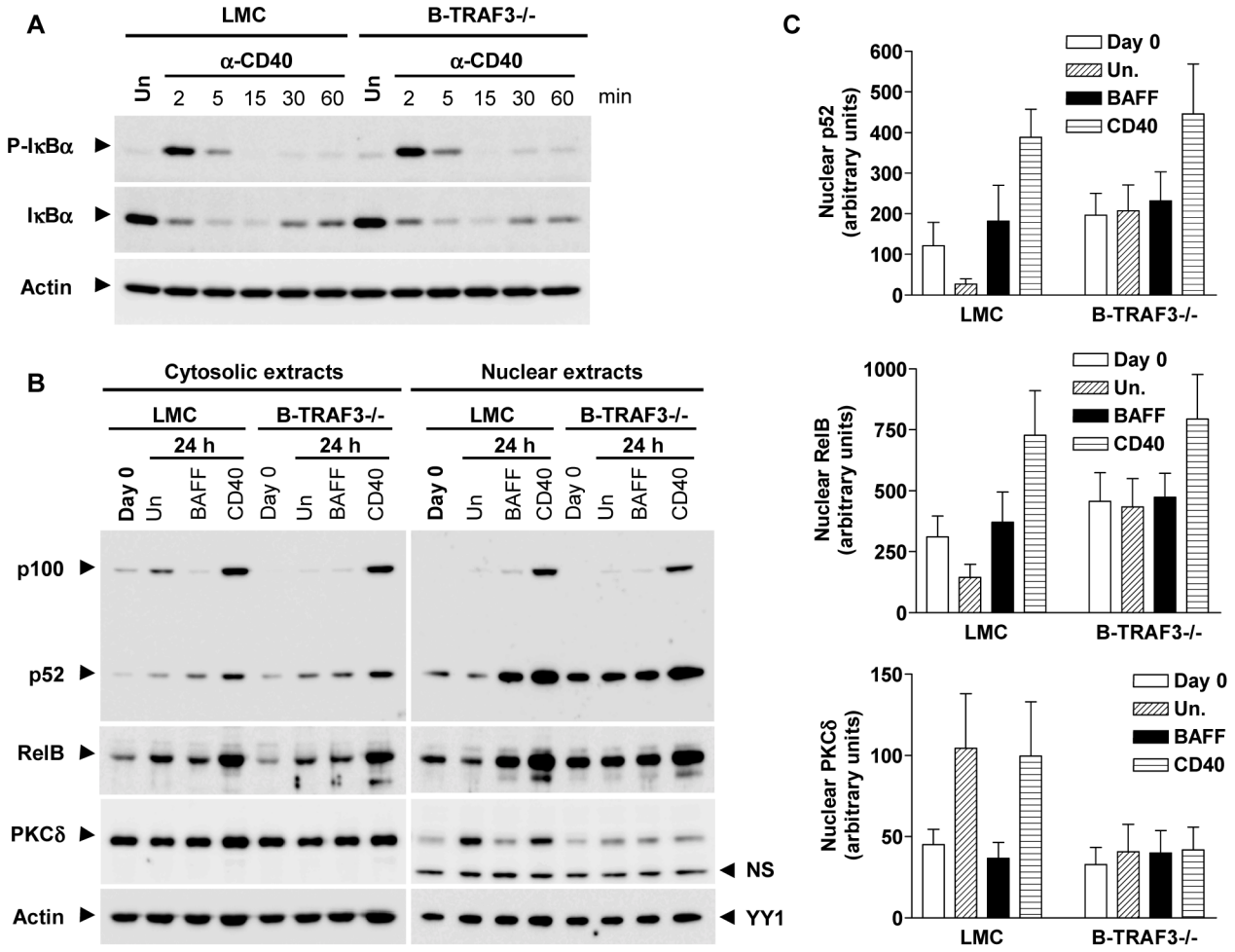

Figure 5. Increased NF-κB2 activation and decreased nuclear PKCδ in TRAF3$^{-/-}$ B cells

Resting splenic B cells were purified from 10- to 12- week-old LMC and B-TRAF3$^{-/-}$ mice, and cultured *ex vivo* in the absence or presence of 2 μg/ml anti-CD40 Abs for indicated times. (**A**) NF-κB1 activation. Total cellular lysates were immunoblotted for phosphorylated (P-) or total IκBα, followed by actin. (**B**) NF-κB2 activation and PKCδ nuclear translocation. Cytosolic and nuclear extracts were immunoblotted for NF-κB2 (p100/p52), RelB, and PKCδ, followed by actin (used as loading control for cytosolic proteins) or YY1 (used as loading control for nuclear proteins). (**C**) Quantitation of nuclear p52, RelB and PKCδ protein levels. Nuclear p52, RelB and PKCδ bands on immunoblots (right panel of B) were quantitated using a low-light imaging system, and the results presented graphically. The amount of p52, RelB or PKCδ in each lane was normalized to the intensity of the corresponding YY1 band. The graph depicts the results of 3 independent experiments (mean ± SEM).

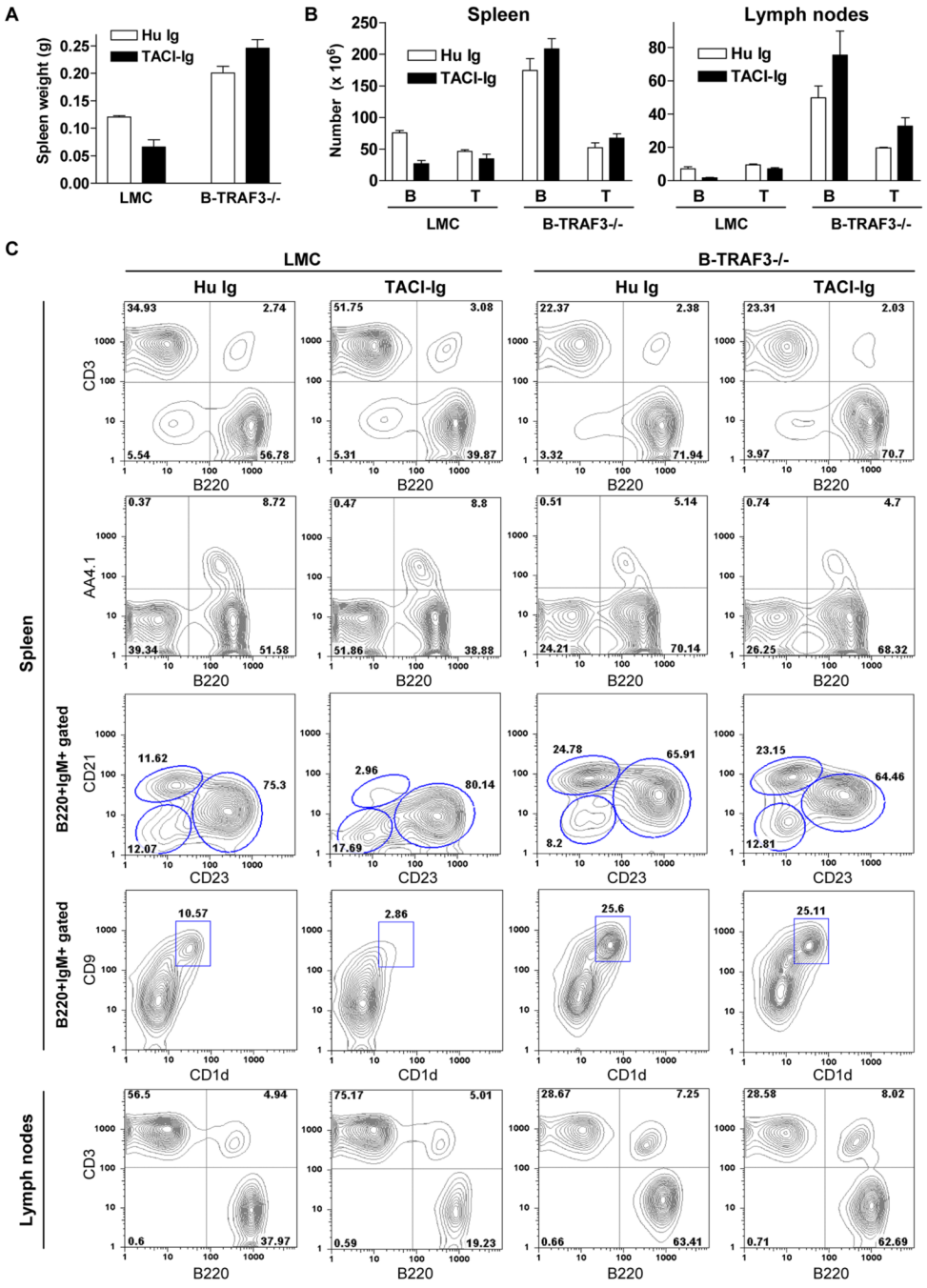

Figure 6. Independence of TRAF3$^{-/-}$ B cell hyperplasia from BAFF/APRIL signaling

LMC and B-TRAF3$^{-/-}$ mice (10 weeks old, n=2 for each group) were i.p. injected with TACI-Ig or a control human Ig Fc (Hu Ig). (**A**) Unreduced spleen weight of B-TRAF3$^{-/-}$ mice after *in vivo* administration of TACI-Ig. The graph shows the results of two independent experiments (mean ± SE). (**B**) Failure of TACI-Ig to decrease the percentages and numbers of B cells in spleen and LN of B-TRAF3$^{-/-}$ mice. B and T cells were identified by FACS analysis using B220 and anti-CD3. The graph depicts the results of two independent experiments (mean ± SE). (**C**) Representative FACS histograms or contour plots of splenocytes and LN cells after TACI-Ig or Hu Ig administration. FACS profiles were scatter-gated on single lymphocytes. Similar results were observed in a second experiment.

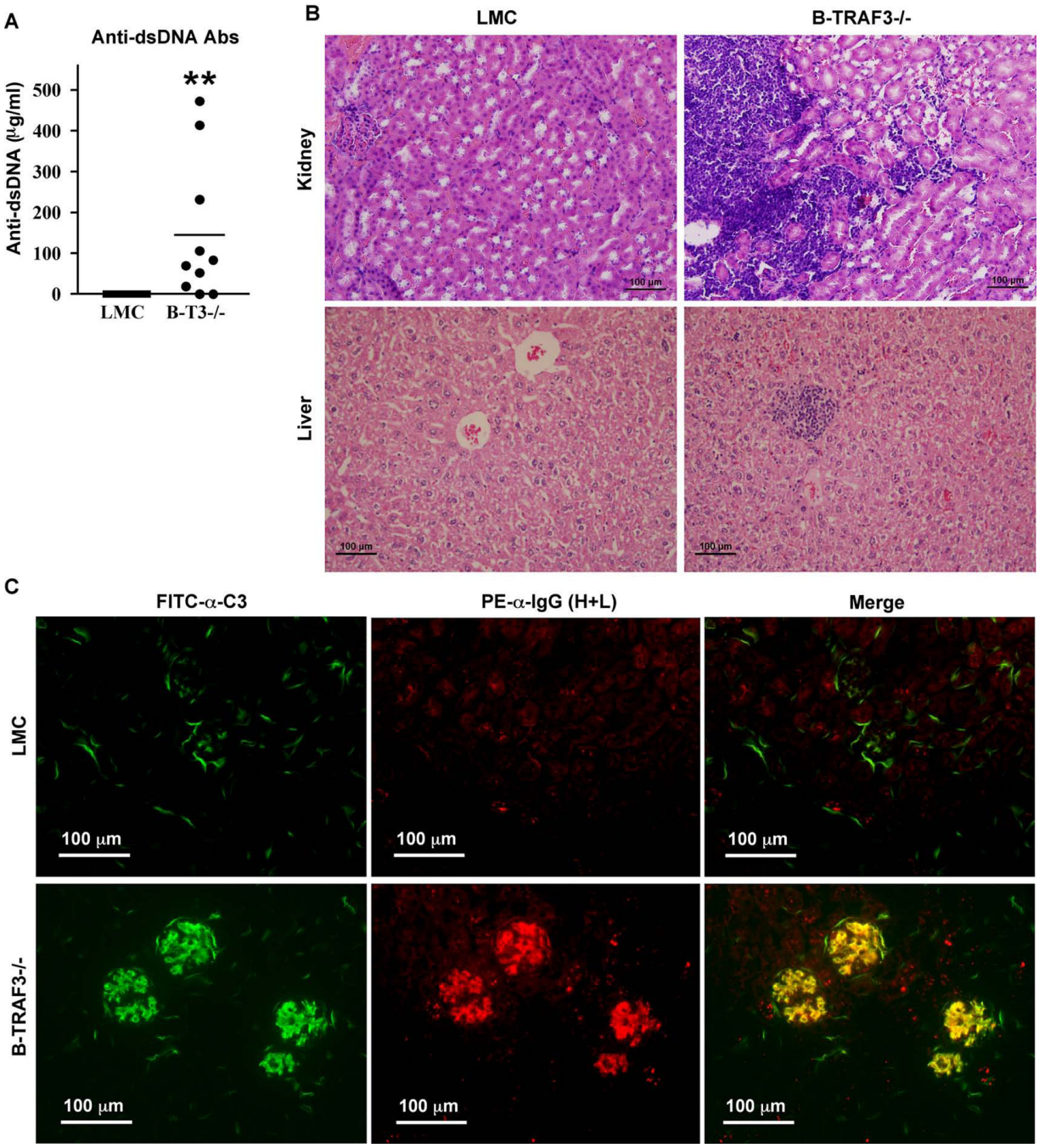

Figure 7. Autoimmune manifestations in B-TRAF3$^{-/-}$ B mice

(**A**) Anti-dsDNA autoantibodies in sera of B-TRAF3$^{-/-}$ mice. Sera from naïve LMC and B-TRAF3$^{-/-}$ mice (n=10 for each group) were tested for anti-dsDNA autoantibodies by ELISA. Mice analyzed were 10 to 12 weeks old. **, highly significantly different from LMC (*t*-test, $P<0.001$). (**B**) Lymphocyte infiltrations in kidney and liver of B-TRAF3$^{-/-}$ mice. Microsections of kidneys and livers were stained with hematoxylin and eosin, and representative micrographs of LMC and B-TRAF3$^{-/-}$ mice are shown for comparison. (**C**) Immune complex deposition in kidney of B-TRAF3$^{-/-}$ mice. Cryosections of kidneys were blocked and stained with anti-C3-FITC (green, micrographs shown in the left panel) and anti-IgG (H+L)-PE (red, micrographs shown in the middle panel). The right panel shows the overlay of C3 and IgG (H+L) staining,

and yellow color indicates co-localized staining. Mice analyzed in (B) and (C) were 9-12 months old, and similar results were observed in two additional experiments.